Layover Separation in Airborne Single Pass Multi-baseline InSAR Data Based on Compressive Sensing

Michael Schmitt, Uwe Stilla
Photogrammetry & Remote Sensing, Technische Universitaet Muenchen (TUM), Munich, Germany

Abstract

The analysis of urban areas by means of very high resolution SAR remote sensing always has to deal with effects caused by the side-looking imaging geometry. Recently, the separation of scatterers that collapsed in one layover affected resolution cell has been thoroughly investigated for multi-baseline InSAR configurations. While most of the time repeat pass data acquired by satellite SAR systems has been in the focus of research, this paper deals with airborne single pass multi-baseline data in the millimeter wave domain. Based on simulated data, the applicability of compressive sensing is investigated and adapted to a single pass system with four receiving channels

1 Introduction

The analysis of urban areas by very high resolution interferometric SAR remote sensing has been an important research topic for some years now [1], [2]. Especially the side-looking imaging geometry inherent to conventional SAR sensors leads to challenging effects like shadowing and layover. While radar shadow can be tackled by making use of multi-aspect configurations [3], multi-baseline data has to be used in order to separate information from different scatterers contained in one layover affected resolution cell [4].

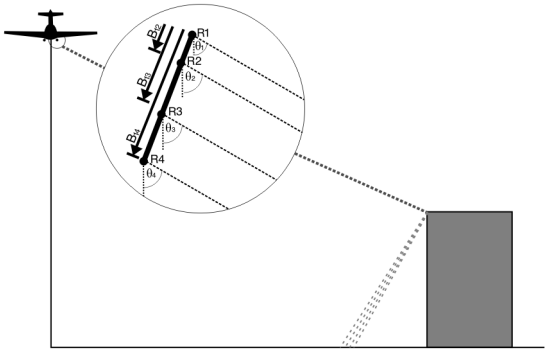

Figure 1 MEMPHIS multi-baseline InSAR configuration with four receiving channels (R1-R4)

2 Single Pass Multi-baseline InSAR System

2.1 MEMPHIS System Description

MEMPHIS is an acronym for **M**illimeterwave **E**xperimental **M**ultifrequency **P**olarimetric **H**igh Resolution **I**nterferometric **S**ystem and was developed by the Research Institute for High-Frequency Physics and Radar Techniques of the FGAN, now Fraunhofer FHR [5]. Although it can be operated in different modes, for the reflections in this paper only the *35 GHz* (Ka band) configuration with a bandwidth of *800 MHz* is considered. The resulting pixel spacing of the data is *5 cm* in azimuth and *19 cm* in range direction.
The interferometer consists of one emitting horn and four receiving channels with a maximum baseline of *27.5 cm*, which corresponds to a height ambiguity of about *55 m* in standard interferometric processing. An illustration of this single pass multi-baseline InSAR system can be seen in Fig. 1.
Since MEMPHIS is still an experimental system, it is commonly mounted on a C-160 Transall and flown at low altitudes of about *300* to *1000 m* above ground level. In combination with a mean viewing angle of about *60°*, this leads to a typical swath size of *600 m* in range direction and up to *3000 m* in azimuth direction.

2.2 Layover

While the single pass nature generally eases interferometric analysis – e.g. no atmosphere effects and no temporal decorrelation have to be considered – the low flying height and therefore shallow off-nadir angle lead to large shadow areas and a compression of information into small layover patches. In order to give a coarse approximation, the ground area affected by layover can be calculated by

$$l_{Layover} = \cot(\theta) \cdot h\,. \qquad (1)$$

With the above-mentioned off-nadir angle $\theta = 60°$ and a typical building height $h = 15\ m$, the complete back-

scattering information of the building façade mixes with about *8.7 m* of ground in front of the building (cf. Fig. 1) – equivalent to about 40 pixels in the slant range image. Therefore, methods for layover separation are needed.

2.3 Multi-baseline Interferometry

It is well-known that the expected height resolution of multi-baseline InSAR systems is given by

$$\rho_h = \frac{\lambda R}{2\Delta B}\sin(\theta) \tag{2}$$

corresponding to a Cramer-Rao bound for the height estimates of

$$\sigma_h = \frac{\lambda \cdot R\sin(\theta)}{2\pi\sqrt{N}\cdot\sqrt{2SNR}\cdot\sigma_B} \tag{3}$$

where λ is the wavelength, R the slant range distance, ΔB the maximum baseline span, σ_B the standard deviation of the baseline distribution, N the number of channels and $\sin(\theta)$ the elevation to height conversion factor [6].
For the MEMPHIS configuration with $N = 4$, this results in a theoretical height resolution of $\rho_h \approx 21\ m$ and a theoretically achievable minimum standard deviation of $\sigma_h \approx 1.7\ m$ for an $SNR = 10\ dB$.
In [7] it has been shown that single pass systems are able to retrieve the heights of $K = N - 1$ scatterers, which means that the interferometric MEMPHIS configuration should be able to separate the information of up to 3 height contributions within one resolution cell. Since, however, the available height resolution is quite low, methods capable of super-resolution are needed.

3 Layover Separation Using Compressive Sensing

3.1 Standard Compressive Sensing

A very promising super-resolution method for the separation of several height contributions within a layover resolution cell is compressive sensing (CS) [8]. Its applicability for SAR tomography problems was first proven using repeat pass TerraSAR-X data [9].
The method is based on the system imaging model

$$\mathbf{g} = \mathbf{A}\mathbf{x} + \mathbf{n}\,, \tag{4}$$

where **g** is the measurement vector containing N single look complex observations, **A** is the *N x L* steering matrix containing the mapping of *L* discretized height values, **x** is the discrete and sparse reflectivity vector corresponding to the searched height profile, and **n** is the additive noise term.
The *N x L* elements of the steering matrix are given by

$$a_{nl} = \exp\left(-j\frac{2\pi}{\lambda}\cdot\frac{B_{\perp,nl}}{R_n\sin(\theta_{nl})}\right) \tag{5}$$

where $B_{\perp,nl} = B\cos(\theta_{nl} - \alpha)$ is the perpendicular baseline, α the baseline tilt and $\theta_{nl} = \arccos\left((H_n - h_l)/R_n\right)$ the range and height dependent off-nadir angle.
The unknown reflectivity is then estimated using a convex minimum L_1 norm reconstruction [10]:

$$\min\left\|\hat{\mathbf{x}}\right\|_1 \text{ s.t. } \left\|\mathbf{A}\hat{\mathbf{x}} - \mathbf{g}\right\|_2 \le \varepsilon\,. \tag{6}$$

ε is a noise dependent threshold that can be calculated based on singular value decomposition (see section 3.4).
The non-zero elements in the sparse solution vector $\hat{\mathbf{x}}$ correspond to heights that contributed to the observed layover signal.

3.2 Distributed Compressive Sensing

Recently, another method based on the sparsity assumption and the according L_1 norm minimization was adapted to multi-baseline SAR interferometry: Distributed Compressive Sensing (DCS) [11]. The idea behind DCS is the exploitation of the joint sparsity of the reflectivity vectors of neighboring pixels. This is a valid assumption, as long as these pixels show backscattering information of the same structure, which means either only small or preferably adaptive neighborhoods have to be considered.
The *P* observed *N x 1* stack pixels then are combined in a measurement matrix

$$\mathbf{G} = \left[\mathbf{g}_1\ \ \mathbf{g}_2\ \ \ldots\ \mathbf{g}_P\right], \tag{7}$$

while also the *P* unknown *L x 1* reflectivity vectors are concatenated to a reflectivity matrix:

$$\mathbf{X} = \left[\mathbf{x}_1\ \ \mathbf{x}_2\ \ \ldots\ \mathbf{x}_P\right]. \tag{8}$$

The optimization problem then becomes

$$\min\left\|\hat{\mathbf{X}}\right\|_{2,1} \text{ s.t. } \left\|\mathbf{A}\hat{\mathbf{X}} - \mathbf{G}\right\|_F \le \varepsilon\,, \tag{9}$$

where $\|\bullet\|_{2,1}$ is the mixed norm summarizing the L_2 norms of all matrix rows and $\|\bullet\|_F$ is the Frobenius norm.
Thanks to the mixed norm that ensures joint sparsity between the reflectivity vectors of the pixels, the solu-

tion will benefit from the mutual support between these sparse vectors.
It has to be noted, however, that **A** in (9) only equals the steering matrix from (4) and (6) if all pixels are located in the same range bin. Otherwise, the observations have to be rephased first [11].

3.3 Multilooking and Compressive Sensing

While in DCS the different pixels are taken to be different samples of the same observation, one could also think about considering them as independent observations of the same backscattering process, a view that is not uncommon in SAR interferometry [12]. The main advantage of this idea is the increase of redundant observations for the L_2 norm minimization part.
In this approach, the basic formulae of section 3.1 are used with the difference that the measurement vector is extended by piling the independent pixel stacks:

$$\mathbf{g}_{ML} = \begin{bmatrix} \mathbf{g}_1 \\ \mathbf{g}_2 \\ \vdots \\ \mathbf{g}_P \end{bmatrix} \tag{10}$$

Of course, the steering matrix has to be concatenated accordingly:

$$\mathbf{A}_{ML} = \begin{bmatrix} \mathbf{A}_1 \\ \mathbf{A}_2 \\ \vdots \\ \mathbf{A}_P \end{bmatrix}, \tag{11}$$

with $\mathbf{A}_1 = \mathbf{A}_2 = \ldots = \mathbf{A}_P$ for all pixels of the same range bin (cf. section 3.2).

3.4 Noise-adaptive Thresholding

According to [13], the noise adaptive threshold ε can be chosen by projecting the observations onto the singular values corresponding to noise space.
First of all, singular value decomposition (SVD) has to be applied to the steering matrix **A**:

$$\mathbf{A} = \mathbf{U}\mathbf{S}\mathbf{V}^T, \tag{12}$$

where $\mathbf{U} = [\mathbf{u}_1 \ \mathbf{u}_2 \ \ldots \ \mathbf{u}_N]$ and $\mathbf{V} = [\mathbf{v}_1 \ \mathbf{v}_2 \ \ldots \ \mathbf{v}_L]$ are unitary matrices containing the left and right singular vectors, respectively, while the main diagonal of **S** contains the non-negative singular values in descending order. These singular values usually can be used to distinguish between signal and noise space. If n_ε is the number of singular values corresponding to noise space, the noise level ε can be calculated by

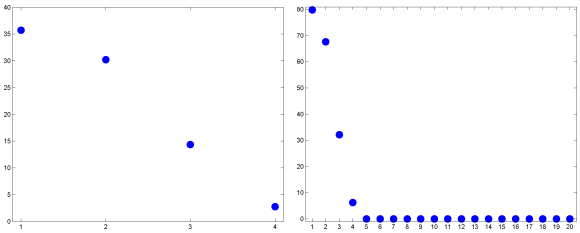

Figure 2 Singular values of the multi-baseline system. Left: single pixel case, right: 5 pixel multilooking case.

$$\varepsilon = \sqrt{\frac{N}{n_\varepsilon} \sum_{n=N-n_\varepsilon+1}^{N} \left|\beta_n^2\right|}, \tag{13}$$

with the afore mentioned projections of observations onto noise space $\beta_n = \mathbf{u}_n^T \mathbf{g} \ \ (n = N - n_\varepsilon + 1 \ \ldots \ N)$.
As can be seen in Fig. 2 (left), none of the only four singular values clearly corresponds to noise space. Since, however, at least one noise singular value is needed in order to determine the noise level always the smallest is chosen for the standard CS method described in section 3.1.
For the methods relying on pixel neighborhoods shown in sections 3.2 and 3.3, $\mathbf{A}_{ML}$ of section 3.3 is decomposed, leading to $4 \cdot P$ singular values, of which always four contain signal information (coming from the four linearly independent lines of $\mathbf{A}_{ML}$), while the rest clearly corresponds to noise space (see Fig. 2 right). The advantage of a clear discriminability of signal and noise space leading to a more robust noise level determination is obvious.

4 Experimental Results

For a first theoretical assessment of the potential of compressive sensing based methods for layover separation in airborne single pass InSAR data, experiments based on simulated resolution cells have been carried out.
The simulations are based on the assumption of two scatterers within one pixel, one at ground level ($h_1 = 0\ m$), one at roof level ($h_2 = 15\ m$). The results of CS, DCS and the multilooking approach to CS (MCS) are plotted for different SNR in Fig. 3, with a utilization of *11* neighboring pixels of the same range bin, which are assumed to contain similar backscattering information. It can clearly be observed that classic CS is not reasonably applicable to multi-baseline InSAR data with only few receiving channels. Both DCS and MCS provide significantly better reconstruction accuracy, especially for low SNR. The lack of sufficient observations, however, can obviously be healed by considering adequate pixel neighborhoods. The dependence on the sample size is shown in Fig. 4. All in all, the multilooking theory leads to slightly better results than distributed compressive sensing.

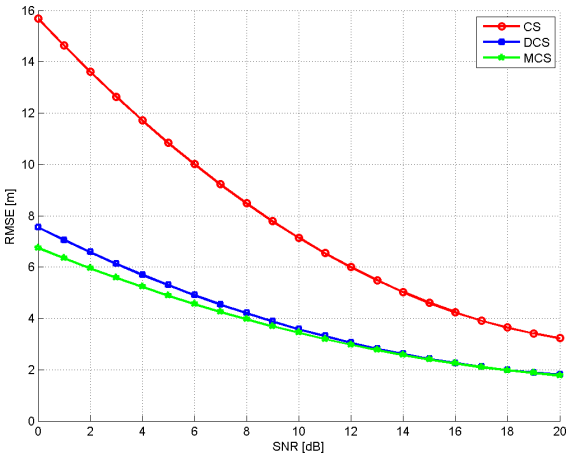

Figure 3 Mean Root Mean Square Error (RMSE) of the reconstructed scatterer heights for growing SNR. Note that only results with correctly estimated sparsity model order ($K = 2$) have been considered.

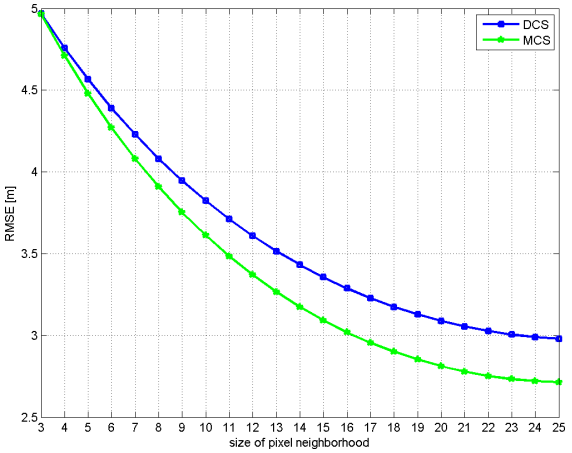

Figure 4 Mean RMSE of the reconstructed scatterer heights for growing size of pixel neighborhood. Again only results with correctly estimated sparsity model order ($K = 2$) have been considered.

5 Conclusion

In this paper it has been shown that compressive sensing based methods can be used for airborne multi-baseline InSAR data with only few receiving channels if the measurements of more than a single resolution cell are used in the estimation process. Future research will have to apply the findings of this paper to real test data. It is worth to be noted that the loss of spatial resolution, which is introduced by considering more than one resolution cell for the estimation process, is not too critical for ultra high resolution airborne SAR data still providing information in the decimeter range even after the combination of several neighboring pixels.

References

[1] Stilla, U., Soergel, U., Thoennessen, U.: *Potential and limits of InSAR data for building reconstruction in built-up areas*. ISPRS Journal of Photogrammetry and Remote Sensing. Vol. 58, No. 1-2, 2003, pp. 113-123

[2] Brenner, A.R., Roessing, L.: *Radar imaging of urban areas by means of very high-resolution SAR and interferometric SAR*. IEEE Transactions on Geoscience and Remote Sensing. Vol. 46, No. 10, 2008, pp. 2971-2982

[3] Schmitt, M., Stilla, U.: *Fusion of multi-aspect InSAR data by simultaneous backward geocoding*. In: Proceedings of Joint Urban Remote Sensing Event, 2011, pp. 53-56

[4] Gini, F., Lombardini, F., Montanari, M.: *Layover solution in multibaseline SAR interferometry*. IEEE Transactions on Aerospace and Electronic Systems. Vol. 38, No. 4, 2002, pp. 1344-1356

[5] Schimpf, H., Essen, H., Boehmsdorff, S., Brehm, T.: *MEMPHIS – a fully polarimetric experimental radar*. In: Proceedings of IEEE International Geoscience and Remote Sensing Symposium, 2002, pp. 1714-1716

[6] Bamler, R., Eineder, M., Adam, N., Zhu, X., Gernhardt, S.: *Interferometric potential of high resolution spaceborne SAR*. Photogrammetrie Fernerkundung Geoinformation. Vol. 2009, No. 5, 2009, pp. 407-419

[7] Lombardini, F., Ender, J., Roessing, L., Galletto, M., Verrazzani, L.: *Experiments of interferometric layover solution with the three-antenna airborne AER-II SAR system*. In: Proceedings of IEEE International Geoscience and Remote Sensing Symposium, 2004, pp. 3341-3344

[8] Baraniuk, R.G.: *Compressive Sensing [Lecture Notes]*. IEEE Signal Processing Magazine. Vol. 24, No. 4, 2007, pp. 118-121

[9] Zhu, X., Bamler, R.: *Tomographic SAR inversion by L1-norm regularization – The compressive sensing approach*. IEEE Transactions on Geoscience and Remote Sensing. Vol. 48, No. 10, 2010, pp. 3839-3846

[10] Grant, M., Boyd, S.: *CVX: Matlab software for disciplined convex programming, version 1.21*. http://cvxr.com/cvx

[11] Aguilera, E., Nannini, M., Reigber, A.: *Multi-signal compressed sensing for polarimetric SAR tomography*. In: Proceedings of IEEE International Geoscience and Remote Sensing Symposium, 2011, 1369-1372

[12] Parizzi, A., Brcic, R.: *Adaptive InSAR stack multilooking exploiting amplitude statistics: A comparison between different techniques and practical results*. IEEE Geoscience and Remote Sensing Letters. Vol. 8, No. 3, 2011, pp. 441-445

[13] Zhu, X., Bamler, R.: *Very high resolution spaceborne SAR tomography in urban environment*. IEEE Transactions on Geoscience and Remote Sensing. Vol. 48, No. 12, 2010, pp. 4296-4308